Front. Optoelectron. China 2010, 3(4): 387–393
DOI 10.1007/s12200-010-0128-3

RESEARCH ARTICLE

Carrier radiation distribution in organic light-emitting diodes

Lei DING (✉), Fanghui ZHANG, Qian JIANG, Honggang YAN, Dinghan LIU

School of Electric and Information Engineering, Shaanxi University of Science and Technology, Xi'an 710021, China

Abstract This paper is based on the analysis of white organic electroluminescent device electroluminescent spectrum to explain the regular pattern of carrier radiation distribution. It has proved electron that is injected from cathode is satisfied with the regularity of radiation distribution on the organic emitting layer. This radiation distribution is related to several factors, such as electron injection capabilities, applied electrical field intensity, carrier mobility, etc. The older instruction design is ITO/2-TNATA/NPB/ADN:DCJTB:TBPe/Alq_3/cathode. Get to change electron injector capabilities through using different cathode and also find electroluminescent spectrum to produce significant changes. Simultaneously, electron radiation quantity has some limitation, and electroluminescent spectrum reflects that spectral intensity does not change anymore when the ratio of cathode dopant reaches a value, namely, the quantity of electron's radiation distribution gets to a saturated state on the organic emitting layer. It also shows the same spectrum variational phenomenon while changing the applied electrical field intensity. To put forward of the carrier radiation distribution is good for organic light emitting diode (OLED) luminescence properties analysis and research.

Keywords carrier radiation distribution, organic light emitting diode (OLED), multiple dopants emission

1 Introduction

Organic light emitting diodes (OLEDs) have attracted considerable attentions due to their highly promising use in full-color flat-panel displays, liquid-crystal-display backlighting, and area illumination [1]. The mechanism for electroluminescence in OLEDs differs in detail from conventional devices made from inorganic semiconductors, in which photon production occurs through the radiative recombination of charged polaron excitons. Electrons and holes, injected from the contacts into the organic layer, form negatively and positively charged polarons in the organic layer. These polarons migrate under the influence of the applied electric field, forming a polaron exciton with an oppositely charged species and subsequently undergoing radiative recombination [2,3]. Both band-based models and exciton-based models have been proposed to explain recent measurements. Then, the mechanism of carrier injection have been put forward; the mechanism include carrier tunneling, interfacial dipoles, interface chemistry, etc. [4–8]. The carrier radiation distribution has been used in other fields [9]; yet, the ideal of carrier radiation distribution in the OLEDs was not put forward so far.

The carrier radiation distribution mechanism has been proposed to explain recent measurements. Support for the mechanism comes from the following:

1) It helps analyze the transport effects of electron and hole within material in the device and then explain the distribution of carriers for the device performance.

2) Increase the carrier intensity within the device, thus increasing the probability of exciton formation to increase the brightness of light-emitting device.

3) Adjust the balance of electron and hole transport to avoid or reduce a weak current induced fluorescent quenching.

In this paper, we presented the mechanism of electron radiation distribution studied by electroluminescent (EL) spectrum and the Commission Internationale de L'Eclairage (CIE) color coordinates and discussed the change in the spectra of the white organic lighting emitting diodes (WOLEDs). Due to the ultrathin profile of the organic layers, we cannot detect the number of electrons in the organic layer. In this study, we developed a white OLED featuring multiple dopants emission layers by separating the recombination zones into red-, green-, and blue-emitting layers [10]. The cathode plays an important role in the overall performance of OLEDs. The paper investigated devices with different cathode for electronic radiation distribution in the triply doped structure. In these devices, the anodes and hole transport layers are the same so that the

Received September 7, 2010; accepted September 28, 2010

E-mail: ostrich132@163.com

current-density-voltage (*J-V*) characteristics are determined by the electron injection efficiency. The theoretical mechanism proposed is helpful to analyze and study the correlation characteristic of OLED and is a good reference for further study of carrier injection mechanism.

2 Experimental details

We report in this paper, using triply doped structure, the structure of this device as follows:

2-TNATA (15 nm)/NPB (20 nm)/ADN:TBPe (2 wt%): DCJTB (1 wt%) (30 nm)/Alq_3 (20 nm)/cathode.

The organic layer stack consists of 4,4′,4″-tris[2-naphthyl(phenyl)amino]triphenylamine (2-TNATA) as the anode buffer layer, *N*,*N*′-bis(naphthalen-1-yl)-*N*,*N*′-bis(phenyl)ben-zidine (NPB) as the hole transport layer (HTL), 9,10-di(2-naphthyl)anthracene (ADN) as the blue emitter, and tris-(8-hydroxyquinoline) aluminum (Alq_3) as the electron transporting layer (ETL).

4-(dicyanomethylene)-2-t-butyl-6(1,1,7,7-tetramethyl-julolidyl-9-enyl)-4H-pyran (DCJTB), 2,5,8,11-tetra-tertbutylperylene (TBPe), Alq_3 are red, blue, and green dyes, respectively. To investigate different cathode for the electron radiation distribution, we constructed two kinds of cathode devices: LiF/Al and Ca:Al alloy. The structures are given as follows:

2-TNATA (15 nm)/NPB (20 nm)/ADN:TBPe (2 wt%): DCJTB (1 wt%) (30 nm)/Alq_3 (20 nm)/LiF (1 nm)/Al (100 nm)

2-TNATA (15 nm)/NPB (20 nm)/ADN:TBPe (2 wt%): DCJTB (1 wt%) (30 nm)/Alq_3 (20 nm)/Ca:Al (*x* wt%) (100 nm)

Figure 1 shows the molecular structure of the used organic materials and the configuration of the devices.

OLEDs were fabricated on indium-tin-oxide (ITO)-coated glass substrates with a nominal sheet resistance of 20 Ω/sq. Substrates were cleaned in ultrasonic baths of acetone, isopropyl alcohol, and methanol, dried in a stream of nitrogen, and then treated with a plasma etcher

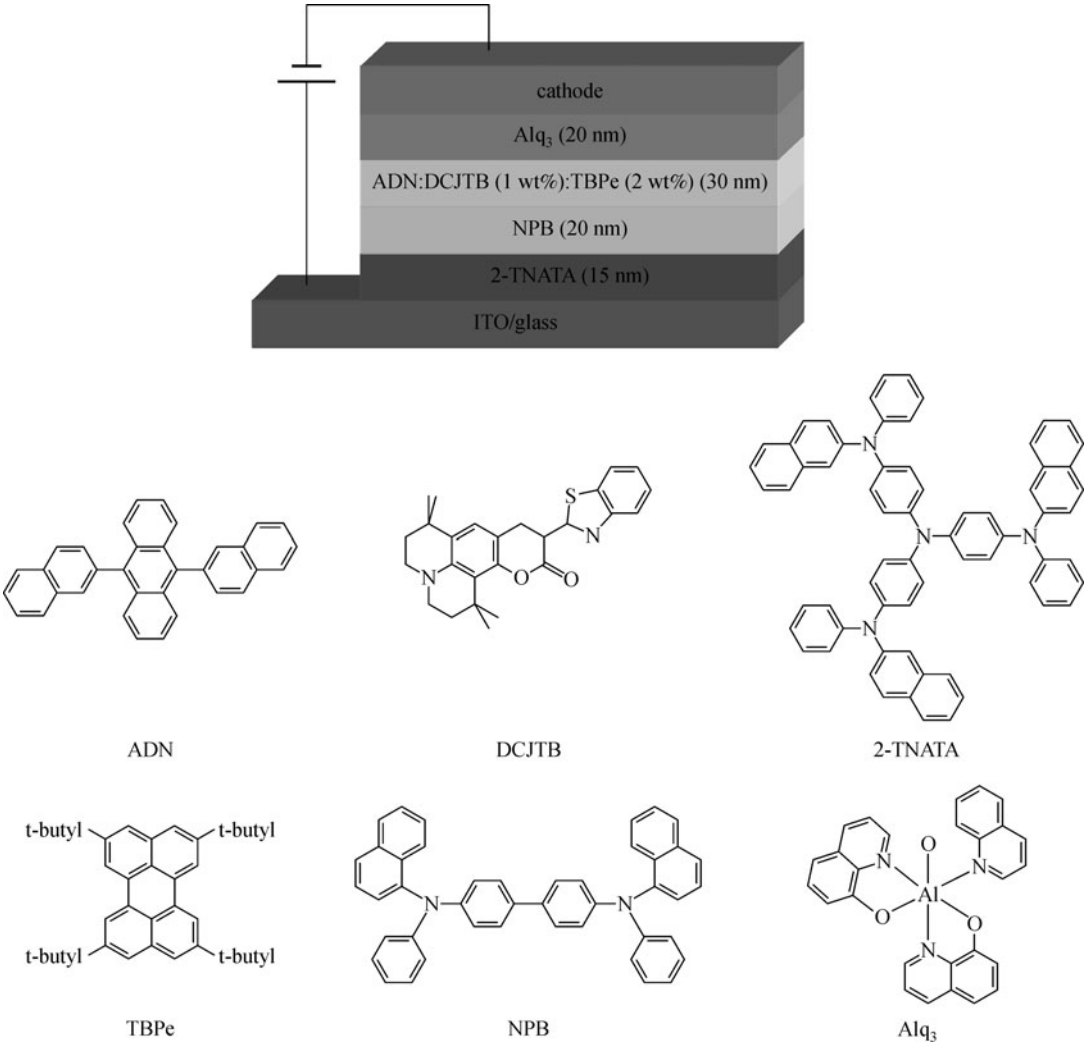

Fig. 1 Configurations of devices and molecular structures of organic materials used

immediately prior to device fabrication. The organic layers and the cathode were sequentially deposited by conventional vacuum vapor deposition in the same chamber. The composite film was prepared from simultaneous co-deposition of host and dopants from three separate sources. The concentrations (wt%) of the dopant materials were estimated from the rations of the evaporation rates. The pressure of the chamber was 10^{-6} Torr without breaking the vacuum. The thickness of the organic layers was measured by using quartz-crystal monitors. Typically, organic layers 2-TNATA, NPB, emitting material layer (EML), Alq_3, and compound cathode LiF/Al were thermally deposited on the substrates treated at a rate of 0.3 nm/s and 1 nm/s, respectively. The active area of the OLED was 2.1 cm^2. The devices were not encapsulated, and the measurements were carried out at room temperature under ambient conditions.

The electroluminescent (EL) spectrum and the CIE color coordinates were measured by PMS-80 spectra scan; the current, voltage, and luminance were performed using a PS-3003D source meter and a ST-900B luminance meter.

3 Results and discussion

Figure 2 shows the dependence of current density and luminance on different voltages.

It can be seen in Fig. 2 that with the addition of Ca into Al cathode, the current density of the devices were sharply increased by increasing the concentration of Ca in Al from 5 wt% to 15 wt%. Apparently, the 20 wt% Ca:Al device was the lowest current density with the same voltage. Because the work function of the cathode was decreased with increasing the concentration of Ca, the alloy is believed to lower injection barrier and increase the electron injection to Alq_3, so the current density was continuously increased. However, the 20 wt% Ca:Al device has a higher barrier height because the Ca diffuses and reacts with Alq_3 to form CaO at the interface [11], crystallization of the Alq_3 layer [12], and delamination at the interface [13]. LiF cathode device shows higher luminance than Ca:Al alloy cathode, as shown in the inset of Fig. 2. Obviously, the luminance of Ca:Al alloy device were increased by increasing the concentration of Ca from 5 wt% to 15 wt%, and the luminance of 20 wt% Ca:Al alloy device shows the lowest luminance. This implied that the 20 wt% Ca:Al alloy device had lower efficiency.

Figure 3 gives the dependences of efficiency on the current density of five devices. It can be seen that the device with LiF cathode shows the highest efficiency and a flat dependence of efficiency on the current density, e.g., a weak current induced fluorescent quenching [14]. It reached a current efficiency of 12.7 cd/A and a power efficiency of 2.92 lm/W.

As shown in Fig. 4, the energy levels of TBPe located between that of ADN and DCJTB, its absorption spectrum overlays with the emission spectrum of and, as well as its emission spectrum overlays with the absorption of DCJTB

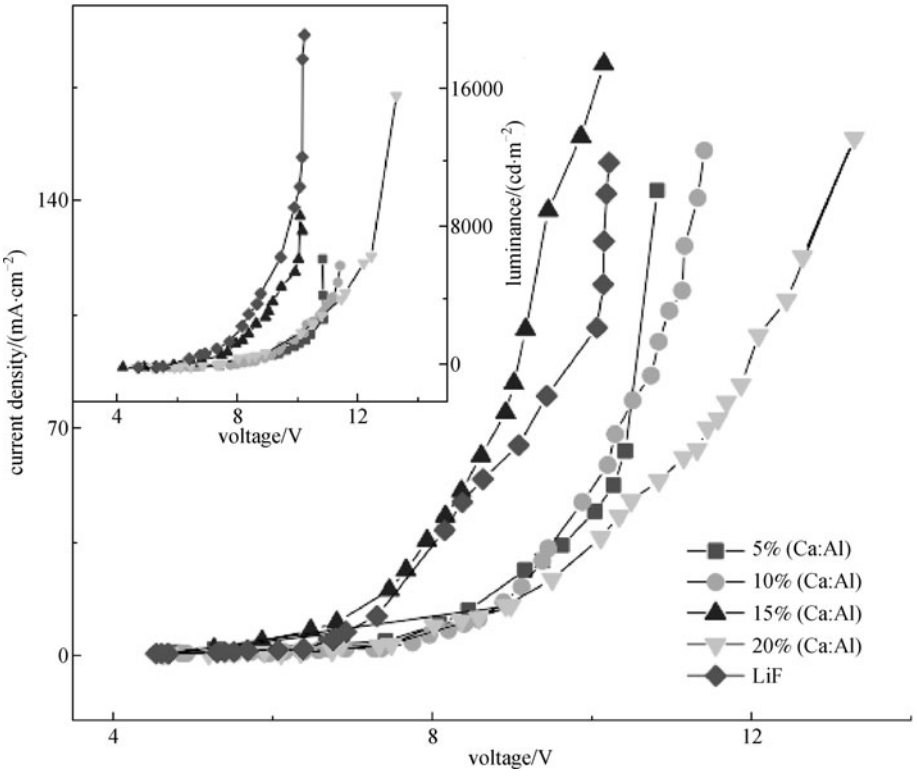

Fig. 2 Current density versus voltage and luminance versus voltage for LiF and Ca:Al alloy cathode

[15]. The cascade energy transfer in co-doping system was proved to have higher energy transfer efficiency and reported in other papers [16–19].

Figure 5 gives the absolute spectra of devices with the different concentration Ca:Al alloy devices at 0.02 and 0.04 A. It can be seen that in Fig. 5(a) there is the same increasing tendency at emission of 460 and 490 nm, it shows that the 10 wt% of Ca:Al device has the highest EL intensity and the 20 wt% of the device has the lowest EL intensity. However, the 15 wt% Ca:Al device shows the highest EL intensity at the emission of 573 nm, and the EL intensity of other devices were increased by increasing the concentration of the Ca:Al alloy. These changes can be explained by the mechanism of electronic radiation distribution, it was already reported that the different concentration of Ca:Al alloy cathode shows the different

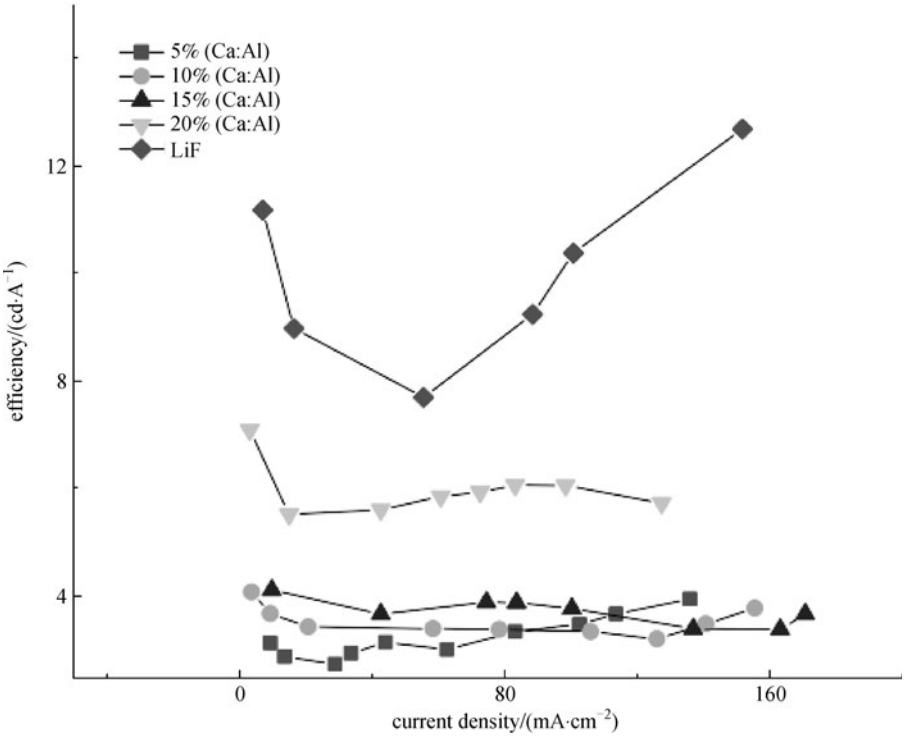

Fig. 3 Efficiency versus current density curves for LiF and Ca:Al alloy cathode

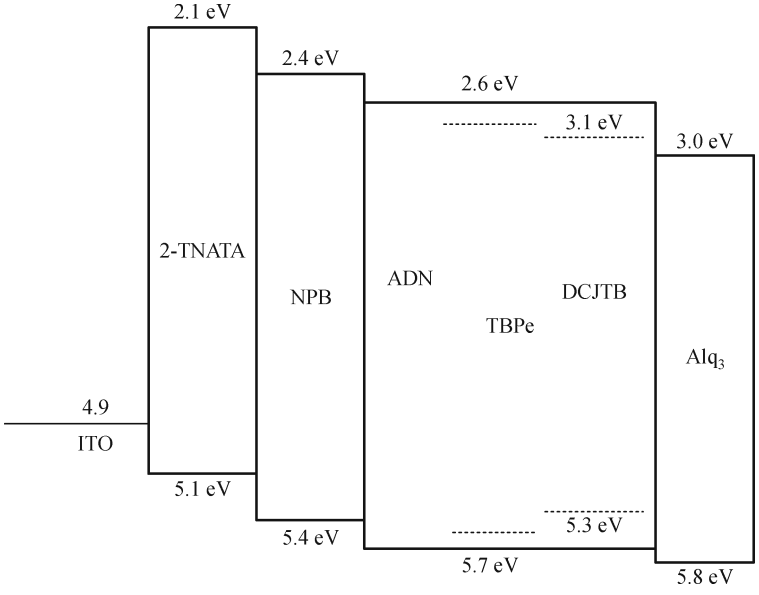

Fig. 4 Energy-level diagram of devices (energy level values of ADN, TBPe, and DCJTB are quoted from Refs. [20,21])

Fermi levels [14], and the organic emitting material has different work function. Therefore, the number of electrons injected from cathode into organic material is not equal. For example, the Fermil level of the 10 wt% of the Ca:Al cathode is closer to lowest unoccupied molecular orbital (LUMO) of Alq_3 (3.0 eV). Therefore, there are more numbers of electrons that radiate into the LUMO of Alq_3 because both of them have a lower barrier height. In this case, more electrons can be injected into the ADN layer as a result of having the same barrier height between the emitting layer and Alq_3. More excitons will be created on the ADN, which will form a relatively high spectral intensity by the emitting radiation. However, the shoulder and the red peak show that lower EL intensity due to existed higher barrier height between cathode and the emitting layer. Therefore, it can clearly analyze spectra variation. The CIE coordinates changed from (0.276, 0.298) to (0.405, 0.396) upon increasing the concentration of the Ca:Al alloy from 5 wt% to 20 wt%. Thus, when the concentration of the Ca:Al alloy was 10 wt%, we obtained near-white light (0.331, 0.353).

Figure 5(b) shows an interesting situation. At the wavelength of ~460 nm, the red peak (5 wt% Ca in Al cathode device) approximately coincides with the green one (10 wt% Ca in Al cathode device), and the light blue and dark blue peaks fit well together. At the shoulder peak (490 nm), these lines have the tendency to follow the descriptions at the left main peak. As for the wavelength of 573 nm, the green peak departs from the red one, and for the meantime, the other two crests coincide with each other. It is difficult to explain the EL spectra. It may be interpreted that the coincidence spectrum is attributed to the electronic radiation distribution that reaches a saturation point.

Figure 6 shows the EL spectra of the four devices with different concentrations of Ca:Al alloy cathode, and the EL spectra of LiF cathode recorded at various driving current. The normalized EL spectra in Fig. 6(a) displays two major emission: one at 490 nm arising from the blue-emitting layer (TBPe) and the other at 573 nm arising from the red-emitting layer (DCJTB). It is obviously found that different concentrations of Ca:Al alloy cathode had different EL intensities. The spectra are analyzed by the electric radiation distribution mechanism, under the same one of the applied electric field intensity; we can see that at peak wavelengths, it shows that the EL intensities of the devices are obviously enhanced with increasing the of concentration Ca:Al alloy cathode at 573 nm. The electronic radiation distribution is influenced by the type of cathode. The amount of electron radiation distributed to the emitting light layer is attributed to the different cathodes.

The normalized EL spectra in Figs. 6(b) and 6(c) show the similar tendency in Fig. 6(a). Different cathode shows different electron injection ability. Therefore, electronic radiation distribution was determined by the molecular structure and the electron mobility of organic material or

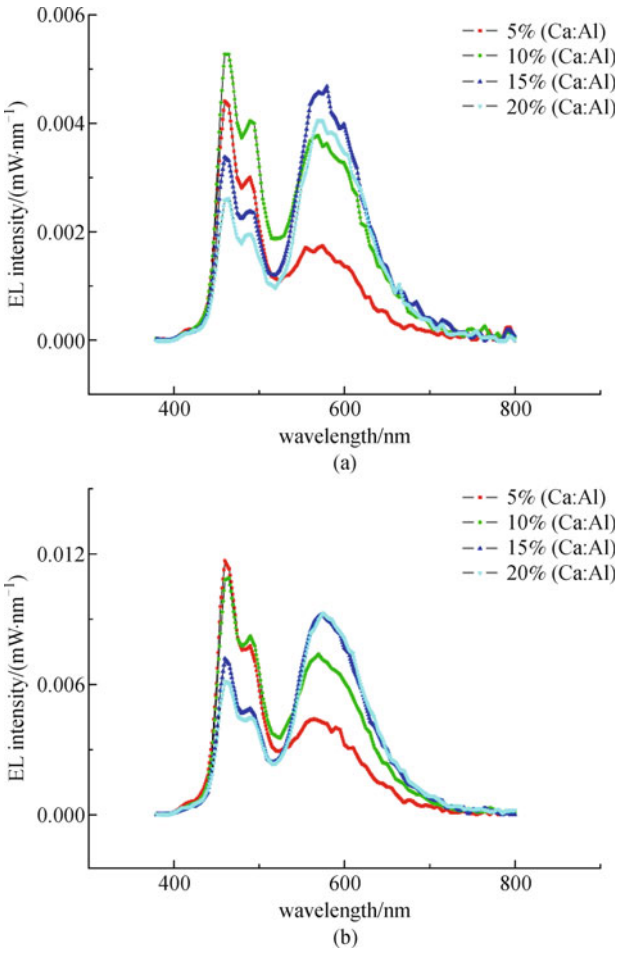

Fig. 5 Absolute EL spectra of Ca:Al alloy cathode at a driving current of (a) 0.02 A and (b) 0.04 A

other factors. In the applications of light emission and photoconduction, the carrier mobility of the organic material plays an important role. Depending on the detailed molecular structures, the morphology, and the electric field intensity applied, the carrier mobility in typical organic semiconductors is in the range of 10^{-7} to 10^{-2} $cm^2/(V \cdot s)$ [22].

Figure 6(d) reveals that the EL spectra of the device with LiF/Al varied significantly over the driving current rang from 0.03 to 0.09 A. We can see that at peak wavelengths, their intensities are dramatically enhanced by increasing the applied electric field. Besides, the EL intensity enhancement of long wavelength is larger than that of short wavelength. The spectra show that most of the electrons are trapped in the DCJTB layer by the effect of applied electric field to form exciton, resulting in the emission of red light. The EL intensity of the blue and green light are weaker than that of the red light. We can obtain that the EL intensity of the devices that have the same cathode increase as the driving current increase. The electrical field intensity plays an important role on the electronic radiation distribution [23].

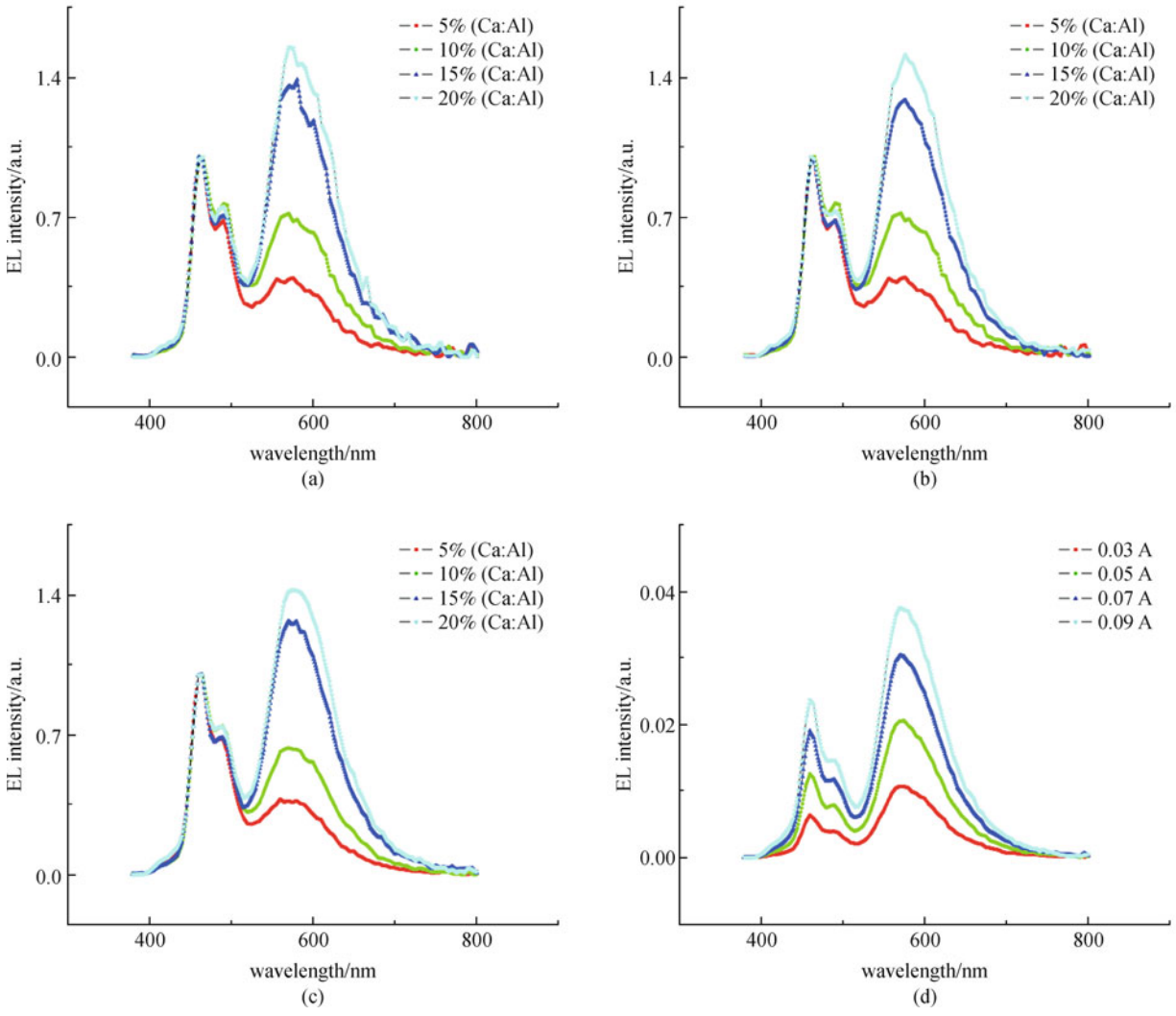

Fig. 6 EL spectra of Ca:Al alloy cathode at a driving current of (a) 0.02 A, (b) 0.04 A, (c) 0.08 A, and (d) the EL spectra of LiF/Al cathode at a driving current of 0.03, 0.05, 0.07, and 0.09 A

4 Conclusion

In conclusion, the paper gives the carrier radiation distribution mechanism that means electron and hole are satisfied with the regularity of radiation distribution on the LUMO and the highest occupied molecular orbital (HOMO) of the organic emitting layer, respectively, under applied electrical field intensity. The carrier radiation distribution mechanism is according to the electroluminescent spectrum of multiple dopants WOLED comes up with regular variation by the changing of the electron injection capability and applied electrical field intensity. In the applied electrical field's role, the electron quantity is satisfied with the distribution regularity that injects each organic emitting layer from the cathode. The more electron radiation distribution quantity, the bigger recombination exciton probability on the organic emitting layer is formed, and the higher the exciton radiation luminous intensity, and the electroluminescent spectrum shows that the organic layer relevant peak is high. The mechanism's proposal contributed to the correlated characteristics of OLED analysis and research and is also a good reference for further study of the carrier injection theory.

Acknowledgements This research was financially supported by the National Natural Science Foundation of China (Grant No. 61076066) and the Doctor Foundation of Shaanxi University of Science and Technology (No. BJ09-07).

References

1. Duggal A R, Shiang J J, Heller C M, Foust D F. Organic light-emitting devices for illumination quality white light. Applied Physics Letters, 2002, 80(19): 3470–3472
2. Hagler T W, Pakbaz K, Voss K, Heeger A J. Enhanced order and electronic delocalization in conjugated polymers oriented by gel

processing in polyethylene. Physical Review B: Condensed Matter and Materials Physics, 1991, 44(16): 8652–8666
3. Bradley D D C, Friend R H. Light-induced luminescence quenching in precursor-route poly(p-phenylene vinylene). Journal of Physics: Condensed Matter, 1989, 1(23): 3671–3678
4. Hung L S, Zhang R Q, He P, Mason G. Contact formation of LiF/Al cathodes in Alq-based organic light-emitting diodes. Journal of Physics D: Applied Physics, 2002, 35(2): 103–107
5. Mori T, Fujikawa H, Tokito S, Taga Y. Electronic structure of 8-hydroxyquinoline aluminum/LiF/Al interface for organic electroluminescent device studied by ultraviolet photoelectron spectroscopy. Applied Physics Letters, 1998, 73(19): 2763–2765
6. Heil H, Steiger J, Karg S, Gastel M, Ortner H, Von Seggern H, Stößel M. Mechanisms of injection enhancement in organic light-emitting diodes through an Al/LiF electrode. Journal of Applied Physics, 2001, 89(1): 420–424
7. Mason M G, Tang C W, Hung L S, Raychaudhuri P, Madathil J, Giesen D J, Yan J, Le Q T, Gao Y, Lee S T, Liao L S, Cheng L F, Salaneck W R, dos Santos D A, Bredas J L. Interfacial chemistry of Alq_3 and LiF with reactive metals. Journal of Applied Physics, 2001, 89(5): 2756–2765
8. Parker I D. Carrier tunneling and device characteristics in polymer light-emitting diodes. Journal of Applied Physics, 1994, 75(3): 1656–1666
9. Hinneburg D, Popp P, Leonhardt J. Radiation-induced charge-carrier distribution in electrical fields. Radiation Physics and Chemistry, 1985, 26(5): 575–577
10. Chang M Y, Wang C H, Lin S C, Chen Y F. High-brightness, high-color-purity, white organic light-emitting diodes featuring multiple emission layers. Journal of Applied Physics, 2009, 105(6): 064318
11. Turak A, Grozea D, Feng X D, Lu Z H, Aziz H, Hor A M. Metal/AlQ_3 interface structures. Applied Physics Letters, 2002, 81(4): 766–768
12. Bu H, Rabalais J W. Structure analysis of O_2 and H_2O chemisorption on a Si{100} surface. Surface Science, 1994, 301 (1–3): 285–294
13. Aziz H, Popovic Z, Xie S, Hor A, Hu N, Tripp C, Xu G. Humidity-induced crystallization of tris (8-hydroxyquinoline) aluminum layers in organic light-emitting devices. Applied Physics Letters, 1998, 72(7): 756–758
14. Luo Y, Aziz H, Popovic Z D, Xu G. Electric-field-induced fluorescence quenching in dye-doped tris(8-hydroxyquinoline) aluminum layers. Applied Physics Letters, 2006, 89(10): 103505
15. Jiang X Y, Zhang Z L, Zhu W Q, Xu S H. Highly efficient and stable white organic light emitting diode with triply doped structure. Displays, 2006, 27(4–5): 161–165
16. Hamada Y, Kanno H, Tsujioka T, Takahashi H, Usuki T. Red organic light-emitting diodes using an emitting assist dopant. Applied Physics Letters, 1999, 75(12): 1682–1684
17. Feng J, Li F, Gao W B, Cheng G, Xie W F, Liu S Y. Improvement of efficiency and color purity utilizing two-step energy transfer for red organic light-emitting devices. Applied Physics Letters, 2002, 81 (16): 2935–2937
18. Lee T W, Park O O, Cho H N, Kim Y C. Cascade energy transfer in dye-doped ternary polymer blend light-emitting diodes. Synthetic Metals, 2002, 131(1–3): 129–133
19. Tallman D E, Vang C, Wallace G G, Bierwagen G P. Direct electrodeposition of polypyrrole on aluminum and aluminum alloy by electron transfer mediation. Journal of Electrochemical Society, 2002, 149(3): C173–C179
20. Zhang Z L, Jiang X Y, Zhao W M, Zhu W Q, Zhang B X, Xu S H. A white organic light emitting diode with improved stability. Journal of Physics D: Applied Physics, 2001, 34(20): 3083–3087
21. Shi J M, Tang C W. Anthracene derivatives for stable blue-emitting organic electroluminescence devices. Applied Physics Letters, 2002, 80(17): 3201–3203
22. Chen B J, Lee C S, Lee S T, Webb P, Chan Y C, Gambling W, Tian H, Zhu W H. Improved time-of-flight technique for measuring carrier mobility in thin films of organic electroluminescent materials. Japanese Journal of Applied Physics, 2000, 39(3A): 1190–1192
23. Seo J H, Seo J H, Park J H, Kim Y K, Kim J H, Hyung G W, Lee K H, Yoon S S. Highly efficient white organic light-emitting diodes using two emitting materials for three primary colors (red, green, and blue). Applied Physics Letters, 2007, 90(20): 203507